Frontiers of Physics
https://doi.org/10.1007/s11467-021-1119-0
Front. Phys.
17(3), 32501 (2022)

RESEARCH ARTICLE

Quantum control with Lyapunov function and bang–bang solution in the optomechanics system

Yu Wang[1,2], Yi-Hao Kang[1,2], Chang-Sheng Hu[1,2], Bi-Hua Huang[1,2], Jie Song[3], Yan Xia[1,2,†]

[1] *Fujian Key Laboratory of Quantum Information and Quantum Optics (Fuzhou University), Fuzhou 350108, China*
[2] *Department of Physics, Fuzhou University, Fuzhou 350108, China*
[3] *Department of Physics, Harbin Institute of Technology, Harbin 150001, China*
Corresponding author. E-mail: [†]*xia-208@163.com*
Received September 29, 2021; accepted October 13, 2021

We propose a quantum control scheme with the help of Lyapunov control function in the optomechanics system. The principle of the idea is to design suitable control fields to steer the Lyapunov control function to zero as $t \to \infty$ while the quantum system is driven to the target state. Such an evolution makes no limit on the initial state and one needs not manipulate the laser pulses during the evolution. To prove the effectiveness of the scheme, we show two useful applications in the optomechanics system: one is the cooling of nanomechanical resonator and the other is the quantum fluctuation transfer between membranes. Numerical simulation demonstrates that the perfect and fast cooling of nanomechanical resonator and quantum fluctuation transfer between membranes can be rapidly achieved. Besides, some optimizations are made on the traditional Lyapunov control waveform and the optimized bang–bang control fields makes Lyapunov function V decrease faster. The optimized quantum control scheme can achieve the same goal with greater efficiency. Hence, we hope that this work may open a new avenue of the experimental realization of cooling mechanical oscillator, quantum fluctuations transfer between membranes and other quantum optomechanics tasks and become an alternative candidate for quantum manipulation of macroscopic mechanical devices in the near future.

Keywords bang–bang solution, quantum control, Lyapunov control, optomechanics system

1 Introduction

As an important platform of quantum mechanics, the quantum optomechanics system has been widely investigated because of its possible applications in quantum communication and quantum information processing [1, 2]. Due to the splendid characteristics, several nontrivial quantum phenomena have been realized in optomechanical systems, including near-ground-state cooling [3, 4], strong-coupling effects [5], squeezing of a mechanical oscillator [6–9], and so on. Utilizing these phenomena, lots of schemes have been proposed to realize quantum information tasks under the optomechanical physical model in the past decades [10–59].

In the quantum information tasks [10–59], cooling a mechanical resonator to its ground state is the foundation and precondition for the rest of work in quantum optomechanics system. How to cool a mechanical resonator has attracted much attention and various schemes have been proposed [11–16]. For example, in 2008, Genes *et al.* provided a general framework to describe cooling of a micromechanical oscillator to its quantum ground state by means of radiation-pressure coupling with a driven optical cavity [11]. Lately, Nunnenkamp *et al.* derived an effective master equation describing two-phonon cooling of the mechanical oscillator and demonstrated how to achieve mechanical squeezing by driving the cavity with two beams [12]. Recently, Peterson *et al.* explored the radiation pressure of light and successfully sideband cooled a micromechanical membrane resonator to the quantum back action limit [14]. Among different kinds of cooling schemes [11–16], the sideband cooling is a common cooling method where the decay rate of the cavity mode should be much less than the mechanical frequency. This is a strict restriction since a high quality factor of the cavity is needed, or the Stokes heating cannot be well suppressed and the cooling comes to nothing. Therefore, the strict restriction is hard to implement in most physical systems since a perfect cavity is difficult to achieve experimentally. So it is hard to find a suitable quantum control method to realize the sideband cooling in most physical systems.

* This article can also be found at http://journal.hep.com.cn/fop/EN/10.1007/s11467-021-1119-0.

On the other hand, some significant schemes have been proposed that it is possible to utilize optomechanical coupling in various applications without cooling the mechanical oscillator to its ground state [44–46]. For example, Dong *et al.* experimentally demonstrated an adiabatic transfer of optical fields between two optical modes of a silica resonator without cooling the mechanical oscillator to its ground state [44]. Garg *et al.* presented a scheme for the adiabatic transfer of average fluctuations in the phonon number between two membranes in an optical cavity [45]. Soon after, by invariant-based inverse engineering [46–51], Chen *et al.* designed classical driving fields to transfer quantum fluctuations between two suspended membranes in an optomechanical cavity system [46]. However, these previously reported works [44–46] require a certain initial state or a strict adiabatic condition is satisfied. These constraints may make it difficult to find a suitable quantum control method to realize quantum information processes and obtain a good experimental result.

Thus, whether it is needed to cool the mechanical oscillator to its ground state before we utilize optomechanical coupling in various applications, some constraints always hinder the efficiency of quantum information tasks. So it is important to find a suitable quantum control method in optomechanics system with a wide range of applications and few constraints.

In order to solve the problem, various schemes such as quantum optimal control, quantum Lyapunov control and Lie group decompositions have been used to design control laws to drive quantum systems to target states or to realize some specific operations [36–43, 46, 60–63]. Among these quantum control schemes [36–43, 46, 60–63], quantum Lyapunov control [40–43, 46, 60–63] plays an important role in coherently manipulating quantum systems because it offers a simple and effective way to design control fields. A significant advantage of the Lyapunov method is that the designed control laws would not make the closed-loop system divergent. In addition, the calculation of control fields for Lyapunov control is much easier since it does not need iteration. Another merit of Lyapunov control is that the shape of control fields is flexible. So the Lyapunov control method is a flexible and widely applicable control method.

In quantum Lyapunov control, the function V, called Lyapunov function of quantum states, is specified to design time-varying control fields [60–63]. Then, with the help of control fields, the system converges to the target state given by $\dot{V} = 0$ while V decreases to its minimum value. Lyapunov control scheme does not need to qualify a particular initial state. Besides, different definitions of Lyapunov control function may offer different evolution paths. Thus, manipulating the quantum information process with Lyapunov control is quite flexible.

In this paper, we present a quantum control scheme based on Lyapunov control function $V = Tr(P\rho)$ [60] to manipulate the evolution in the optomechanics system. (We denote the state of the target resonator by ρ and P is an Hermitian operator and assumed to be positive semidefinite in order to satisfy the standard requirement for a Lyapunov control function, $V \geq 0$.) For the sake of convenience, we call this scheme as Lyapunov-based control scheme in the rest of paper. In the scheme, different kinds of quantum information processes can be realized depending on the different definitions of Lyapunov control functions $V = Tr(P\rho)$.

Whereafter, we give two applications to verify the validity of Lyapunov-based control scheme. One is to realize the cooling of mechanical oscillator in linear coupling (LC) circuit. Different from the previously reported sideband cooling schemes [16] where the decay rate of the cavity mode should be much less than the mechanical frequency, the Lyapunov-based control scheme could realize the cooling of mechanical oscillator in the LC circuit with relatively loose parameter selection. The other application is to transfer the quantum fluctuation between two membranes in the cavity optomechanics system. The quantum fluctuations can be coherently and deterministically transferred from one mechanical oscillator to the other with the help of Lyapunov-based control scheme. The evolution process can start with a random initial state and do not have to meet the adiabatic condition. This clearly opens up an avenue of quantum communication between two truly mesoscopic systems. However, cooling of the resonators and the fluctuation transfer between membranes are just two applications of our control method. There are many other aspects to which our scheme can be applied, just like reaching the actual motion of the mechanical membranes [64]. We will give more applications of the control method in the following work.

Furthermore, in the Lyapunov-based control scheme, the amplitude of the control fields $f_n(t)$ is proportional to $T_n(t)$ and will still change during the whole evolution process. For better practical implementation of the scheme, we need to manipulate the control fields at each instance of time and compensate the positive or negative effect caused by time delay in experiments. Therefore, this kind of amplitude may be difficult to control in realistic situations and errors would be introduced in the complexity regulation because the control fields are a continuous function of time. Thus, this is a challenging task for practical applications. To handle this problem, we use the bang–bang solutions [63] of control fields' waveform to optimize the Lyapunov-based control scheme. For convenience, we call this optimized control scheme as bang–bang-based control scheme in the rest of paper. Then, we make a numerical simulation of the fluctuation transfer between two membranes. The simulation shows that it is possible to realize a perfect fluctuation transfer between membranes and the bang–bang-based control scheme makes the evolution time significantly reduced, compared with the Lyapunov-based control scheme. Besides, the optimized design has the bang–bang type control form which may be easier

to realize experimentally [65]. Hence, we hope that this scheme could be a good candidate for the experimental realization of cooling mechanical oscillator, quantum fluctuations transfer between membranes and other quantum optomechanics tasks in the near future.

The paper is organized as follows: In Section 2, we first review the principle of quantum Lyapunov control theory and choose the suitable Lyapunov control function $V = Tr(P\rho)$ to design the Lyapunov-based control fields. To prove the effectiveness of the Lyapunov-based control scheme, two applications are displayed in Section 3 and Section 4, respectively. That is, in Section 3, we consider a LC circuit to cool a nanomechanical resonator to its ground state with the help of Lyapunov-based control scheme. Then, in Section 4, we utilize the Lyapunov-based control scheme to realize the transfer of quantum fluctuations between two membranes in a membrane-in-the-middle (MIM) cavities system. In Section 5, we optimize the Lyapunov-based control scheme with the help of bang–bang solution for better efficiency and experimental feasibility. Finally, we summarize the work in Section 6.

2 The quantum Lyapunov control design

In this section, we propose the quantum control scheme (Lyapunov-based control scheme) based on Lyapunov control function V [42, 60, 63] in the optomechannics system. Firstly, we start with a brief introduction of Lyapunov control function. The definition of quantum Lyapunov control was proposed in the early 2000s as a good candidate for realizing state transfer [40]. Soon after, this strategy has been widely studied both in theory and applications because it offers a simple and effective way to design control fields. Generally, in quantum Lyapunov control theory, the total Hamiltonian can be written in two parts, the free Hamiltonian H_0 and the external control Hamiltonian $H_c(t) = \sum_{n=1}^{k} f_n(t)H_n$ [42, 62]. The Lyapunov control function V of quantum states is specified to design time-varying control fields. These corresponding additional control fields should be designed to ensure $\dot{V} \leq 0$.

However, there are many ways to design control fields to achieve this goal and designing Lyapunov functions from some special geometric or physical meanings is a good approach. Here we consider the following form of Lyapunov control function $V = Tr(P\rho)$, where P is an Hermitian operator and assumed to be positive semidefinite in order to satisfy the standard requirement for a Lyapunov control function, $V \geq 0$ [63].

A controlled quantum system can be modeled in different ways, either as a closed system evolving unitarily governed by a Hamiltonian or as an open system coupling to its environment. We first consider a closed system and its dynamics as Markovian. Therefore the dynamics obeys the Markovian master equation,

$$\begin{aligned} &\dot{\rho} = -\mathrm{i}[H, \rho], \\ &H = H_0 + H_c. \end{aligned} \tag{1}$$

Before we design the control fields, the time derivative of V needs to be calculated as [63]

$$\begin{aligned} \dot{V} &= Tr(-\mathrm{i}P[H_0 + \sum_{n=1}^{k} f_n(t)H_n, \rho]) \\ &= Tr(-\mathrm{i}\rho[P, H_0]) + \sum_{n=1}^{k} f_n(t)Tr(-\mathrm{i}\rho[P, H_n]) \\ &= \sum_{n=1}^{m} f_n(t)T_n(t), \end{aligned} \tag{2}$$

where $T_n(t) = Tr(-\mathrm{i}\rho[P, H_n])$ is a real function of ρ, H_n, and P. For simplification, we have used the assumption that $[P, H_0] = 0$, which can be achieved by constructing P using the eigenvectors of H_0. A simple and conventional way to design the control fields is to let $f_n(t) = -KT_n$ with $K > 0$. In this case, $\dot{V}(\rho) = -\sum_{n=1}^{k} KT_n(t)^2 \leq 0$, so the system converges to the target state ρ_t given by $\dot{V} = 0$ while V decreases to its minimum value.

After introducing the quantum Lyapunov control theory, we will display two applications of Lyapunov-based control scheme in the next two sections.

3 The cooling of resonators

The cooling of resonators has become an active research topic in recent years due to its potential applications in detecting extremely small displacement and observing quantum phenomena of macroscopic mechanical objects [63, 66, 67]. Inspired from the works mentioned in Refs. [62, 63], we will introduce how to utilize the Lyapunov-based control scheme to cool a nanomechanical resonator to its ground state in an open system.

3.1 Physical system and the effective Hamiltonian

When studying the cooling of mechanical resonator, it is not suitable to use the closed system as a cooling environment. This is not a reasonable consideration because the losses and dephasing mechanisms and, most importantly, the flux of energy from the environment to the system have a great influence on the whole cooling process. For more reliable discussion, we restrict our discussion to a N-dimensional open quantum system and consider its dynamics as Markovian.

Consider the circuit in Fig. 1, where a nanomechanical resonator capacitively couples with two charge islands of linear coupling (LC) oscillators, respectively [67]. The nanomechanical resonator interacts with the circuit with

movable membranes. In order to find out more intuitively where the mechanical resonator is, we use a dotted line around the mechanical resonator to emphasize it in Fig. 1. Each LC oscillator includes a capacitor $C_{1(2)}$ and an inductor $L_{1(2)}$. We denote the vibrational displacement of the nanomechanical mode as $x_{1(2)}$ and the annihilation operators for the LC oscillators and the nanomechanical resonators by b_1, b_2 and a, respectively, with $x_{1(2)} = \delta x_0^{1(2)}(a + a^\dagger)$ and $x_0^{1(2)}$ being the quantum displacement of each side. The coupling capacitance can be expressed as $C_{x1(x2)} = C_{x0}^{1(2)} + C'_{x1(x2)}x_{1(2)}$ where $C'_{x1(x2)} = \frac{\partial C_{x1(x2)}}{\partial x_{1(2)}}$. Applying a Lagrangian approach for quantum circuits, the total Hamiltonian of the resonator is given by ($\hbar = 1$) [67]

$$\begin{aligned} H &= H_0 + H_{c1} + H_{c2}, \\ H_0 &= \omega a^\dagger a, \\ H_{c1} &= \frac{(P_{\Phi_1} + v_{c1}C'_{x1}x_1)^2}{2(C_1 + C_{g1} + C_{x0}^1 + C'_{x1}x_1)} + \frac{\phi_1^2}{2L_1}, \\ H_{c2} &= \frac{(P_{\Phi_2} + v_{c2}C'_{x2}x_2)^2}{2(C_2 + C_{g2} + C_{x0}^2 + C'_{x2}x_2)} + \frac{\phi_2^2}{2L_2}, \end{aligned} \tag{3}$$

where ω is the frequency of nanomechanical resonator, P_Φ is the conjugate momentum of the charge island which describes the total charge on the island. This kind of expression is not easy to calculate the effective Hamiltonian of the system, so we use $\Omega_{1(2)}$ to replace $[L_{1(2)}(C_{1(2)} + C_{g1(g2)} + C_{x0}^{1(2)})]^{-1/2}$ to define the frequency of the LC oscillator. In this case, the Hamiltonian of the LC oscillators including the coupling can be rewritten as [67]

$$\begin{aligned} H_{c1} &= \Omega_1 b_1^\dagger b_1 - g_{r1}(a + a^\dagger)b_1 b_1^\dagger - \mathrm{i}g_{l1}(a + a^\dagger)(b_1 + b_1^\dagger), \\ H_{c2} &= \Omega_2 b_2^\dagger b_2 - g_{r2}(a + a^\dagger)b_2 b_2^\dagger - \mathrm{i}g_{l2}(a + a^\dagger)(b_2 + b_2^\dagger), \\ g_{r1} &= \frac{\Omega_1 C'_{x1}\delta x_0^1}{2(C_1 + C_{g1} + C_{x0}^1)}, \\ g_{r2} &= \frac{\Omega_2 C'_{x2}\delta x_0^2}{2(C_2 + C_{g2} + C_{x0}^2)}, \\ g_{l1} &= v_{c1}\sqrt{\Omega_1/2(C_1 + C_{g1} + C_{x0}^1)}(C'_{x1}\delta x_0^1), \\ g_{l2} &= v_{c2}\sqrt{\Omega_2/2(C_2 + C_{g2} + C_{x0}^2)}(C'_{x2}\delta x_0^2), \end{aligned} \tag{4}$$

which includes radiation-pressure-like coupling with the coupling constant $g_{r1(r2)}$ and Bogoliubov linear coupling with the coupling constant $g_{l1(l2)}$. When we choose a suitable voltage of $v_{c1} = v_{c2} = 300\,\mathrm{mV}$, the rate of $g_l/g_r \approx 10^4$ and the radiation-pressure-like coupling can be ignored. Thus, we can deliver the effective Hamiltonian of the system as

$$\begin{aligned} H &= H_0 + H_c(t), \\ H_0 &= \Omega_1 b_1^\dagger b_1 + \Omega_2 b_2^\dagger b_2 + \omega a^\dagger a, \\ H_c(t) &= g_{l1}(t)(b_1 + b_1^\dagger)(a + a^\dagger) \\ &\quad + g_{l2}(t)(b_2 + b_2^\dagger)(a + a^\dagger), \end{aligned} \tag{5}$$

where $(b_1 + b_1^\dagger)$, $(b_2 + b_2^\dagger)$ and $(a + a^\dagger)$ are the position operators of the LC oscillators and the nanomechanical resonator, respectively. One can modify the coupling rate $g_{l1(l2)}(t)$ by changing the voltage of the LC circuit [66, 67].

Therefore the dynamics obeys the Markovian master equation

$$\begin{aligned} \dot\rho &= -\mathrm{i}[H, \rho] + \mathcal{P}, \\ \mathcal{P} &= \kappa_{b_1}\bar n\mathcal{L}(b_1^\dagger) + \kappa_{b_1}(\bar n + 1)\mathcal{L}(b_1) \\ &\quad + \kappa_{b_2}\bar n\mathcal{L}(b_2^\dagger) + \kappa_{b_2}(\bar n + 1)\mathcal{L}(b_2) \\ &\quad + \kappa_a\bar n\mathcal{L}(a^\dagger) + \kappa_a(\bar n + 1)\mathcal{L}(a), \\ H &= H_0 + H_c(t), \\ \mathcal{L}(o) &= 2o\rho o^\dagger - o^\dagger o\rho - \rho o^\dagger o, \end{aligned} \tag{6}$$

where κ_{b_1}, κ_{b_2} and κ_a are the decay rate of the LC oscillators and the nanomechanical resonator, respectively. Here, $\bar n$ represents the temperature of the thermal bath coupled to the LC oscillators and the nanomechanical resonator.

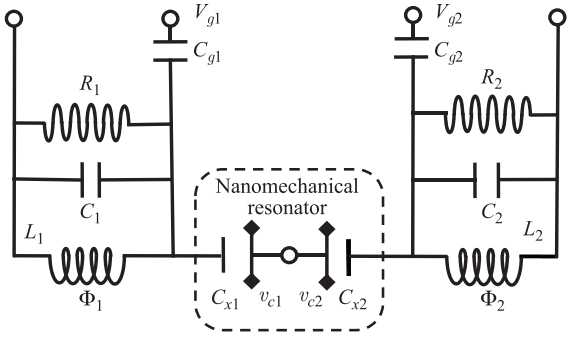

Fig. 1 Schematic circuits of a nanomechanical resonator capacitively linear coupling with a LC oscillator and the resonator is indicated as a bar with two contacts. The resonator interacts with the circuit with a movable membrane. We denote the vibrational displacement of the nanomechanical mode as x and the annihilation operators for the nanomechanical resonator and LC oscillator by b_1 and b_2, respectively, with $x = \delta x_0(a + a^\dagger)$ and x_0 being the quantum displacement. The coupling capacitance can be expressed as $C_x = C_{x0} + C'_x x$ where $C'_x = \frac{\partial C_x}{\partial x}$.

3.2 Corresponding Lyapunov control function and control fields

For the sake of convenience, we denote the state of the target nanomechanical resonator by ρ and use this setting

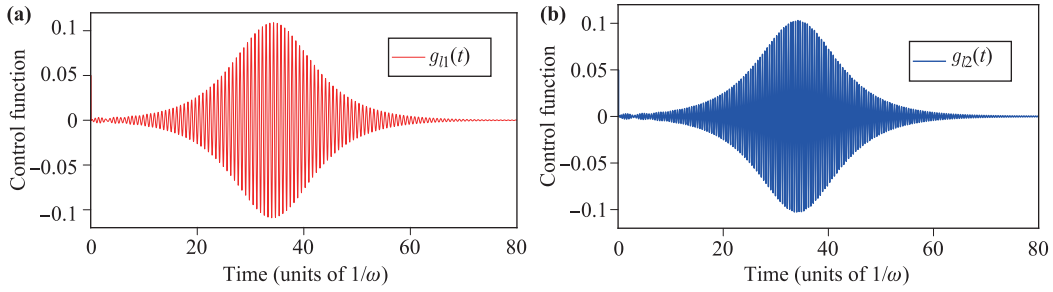

Fig. 2 The intensity of control fields versus time for the Lyapunov-based control scheme to cool a nanomechanical resonator to its ground state. The corresponding parameters are $\omega = 50\,\mathrm{MHz}$, $\Omega_{b1} = 10\omega$, $\Omega_{b2} = 15\omega$, $g_1 = g_2 = 0.05\omega$, $K = 0.01$, $\bar{n} = 1$, $\kappa_{b1} = \kappa_{b2} = \kappa_a = 10^{-5}\omega$. **(a)** The control function $g_{l1}(t)$ versus time. **(b)** The control function $g_{l2}(t)$ versus time.

in the rest of paper. Based on the Lyapunov function $V = Tr(P\rho)$ and the Hamiltonian in Eq. (5) where the free (internal) Hamiltonian is $H_0 = \Omega_1 b_1^\dagger b_1 + \Omega_2 b_2^\dagger b_2 + \omega a^\dagger a$. Similar to Ref. [63], here we set the Hermitian operator P as $P = a^\dagger a$, the corresponding Lyapunov control function is [63]

$$V(\rho) = Tr(a^\dagger a \rho) = \langle n_a \rangle. \tag{7}$$

In this case, we choose the mean phonon number of the target nanomechanical resonator as the Lyapunov control function V, which is non-negative and becomes zero when the target system is cooled to its ground state. Similar to the procedure in Section 2, we should calculate the time derivative of V according to Eqs. (5)–(7),

$$\begin{aligned}
\dot{V} &= Tr\{a^\dagger a(-\mathrm{i}[H_0 + H_c(t), \rho] + \mathcal{P})\} \\
&= f_1(t)T_1(t) + f_2(t)T_2(t) + Tr(a^\dagger a \mathcal{P}), \\
T_1(t) &= Tr\{-\mathrm{i}\rho[a^\dagger a, (b_1 + b_1^\dagger)(a + a^\dagger)]\} \\
&= Tr\{-\mathrm{i}\rho(a^\dagger - a)(b_1 + b_1^\dagger)\}, \\
T_2(t) &= Tr\{-\mathrm{i}\rho[a^\dagger a, (b_2 + b_2^\dagger)(a + a^\dagger)]\} \\
&= Tr\{-\mathrm{i}\rho(a^\dagger - a)(b_2 + b_2^\dagger)\},
\end{aligned} \tag{8}$$

where

$$\begin{aligned}
Tr(a^\dagger a \mathcal{P}) &= Tr[a^\dagger a(\kappa_a \bar{n}\mathcal{L}(a^\dagger) + \kappa_a(\bar{n}+1)\mathcal{L}(a)] \\
&= Tr[2\kappa_a \bar{n}\rho a a^\dagger - 2\kappa_a(\bar{n}+1)\rho a^\dagger a] \\
&= Tr[2\kappa_a \rho(\bar{n} - a^\dagger a)].
\end{aligned} \tag{9}$$

It is noticed that when we realize the cooling of resonator, the temperature of the thermal bath $\bar{n}$ is generally considered to be higher than the temperature of the target resonator $\langle a^\dagger a \rangle$. So the term $Tr[2\kappa_a \rho(\bar{n} - a^\dagger a)]$ in Eq. (9) should be a negative number. Then, we set the time-dependent coupling strength as $f_{1(2)}(t) = -KT_{1(2)}(t)$ with K being a positive constant [63]. In this case, the time derivative of Lyapunov control function $\dot{V} = Tr\{a^\dagger a(-\mathrm{i}[H_0 + H_c(t), \rho] + \mathcal{P})\} \leq 0$. Because the time derivative of Lyapunov control function V is less than or equal to zero and we choose the mean phonon number of the target resonator as the Lyapunov control function V, the phonon number of target resonator will decrease monotonically. Meanwhile, the target nanomechanical resonator will be gradually cooled to the ground state. Next we will use the the Markovian master equation in Eq. (6) to perform numerical simulation.

3.3 Analysis and numerical simulations

In this subsection, numerical simulation was used to prove the effectiveness of the cooling of resonators with Lyapunov-based control scheme. The simulations are performed in the Fock space. For the sake of simplicity, here we truncate the Fock space of each oscillator up to 15-Fock-states. In order to choose the suitable phonon number truncation point, we compared the simulations with 20-Fock-state truncation and the simulations with 15-Fock-state truncation, the improvement of 20-Fock-state truncation is not significant, so the simulations with 15-Fock-state truncation are reasonable.

Firstly, we assume the target nanomechanical resonator is initially in a thermal state with average phonon number $\langle n_{b_1} \rangle = 3$ and the auxiliary system is prepared in its ground state. With suitable parameters are chosen as $\omega = 50\,\mathrm{MHz}$, $\Omega_{b1} = 10\omega$, $\Omega_{b2} = 15\omega$, $g_1 = g_2 = 0.05\omega$, $K = 0.01$, $\bar{n} = 1$, $\kappa_{b1} = \kappa_{b2} = \kappa_a = 10^{-5}\omega$, the nanomechanical resonator can be rapidly cooled to its ground state.

The corresponding Lyapunov control fields versus time are shown in Fig. 2. It is worth noting that to avoid $T_n(t) = 0$ at the initial time, we set the control fields $g_{l1}(t)$ and $g_{l2}(t)$ start with a nonzero small number $g_{l1}(0) = g_{l2}(0) = 0.1\omega = 5\,\mathrm{MHz}$. The red and blue solid lines in Fig. 2 show that the control fields will work during the evolution and gradually vanish in the end. So the system will become stable again.

As shown in Fig. 3, the dash blue line represents the cooling process in a open system. The phonon number $\langle n_a \rangle$ of the nanomechanical resonator begins to decrease

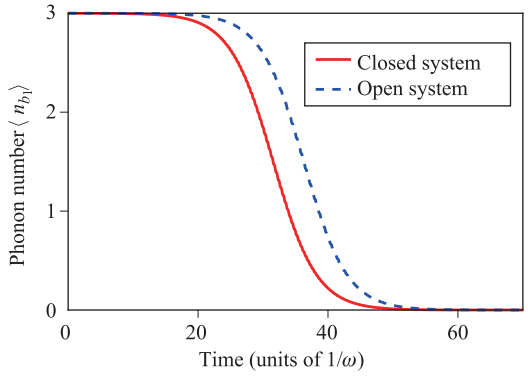

Fig. 3 Phonon number versus time for the Lyapunov-based control scheme to cool a nanomechanical resonator to its ground state. The corresponding parameters are $\omega = 50\,\mathrm{MHz}$, $\Omega_{b1} = 10\omega$, $\Omega_{b2} = 15\omega$, $g_1 = g_2 = 0.05\omega$, $K = 0.01$, $\bar{n} = 1$, $\kappa_{b1} = \kappa_{b2} = \kappa_a = 10^{-5}\omega$.

at $t = 20$ and quickly reduce to $\langle n_s \rangle = 0.05$ at $t = 50$. Comparing the red solid line which represents the cooling process in a closed system and the blue dotted line in Fig. 3, we find that the decay of the mechanical resonator and the thermal noise from environment will affect the cooling process to some extent. However, the cooling of the mechanical resonator with the Lyapunov-based control method can still be achieved when we take the open environment into consideration. The results show that Lyapunov-based control scheme could be a good candidate to cool a nanomechanical resonator to its ground state in current experimental environment.

4 Fluctuation transfer between membranes

In 2010, Tian *et al.* proposed that high-fidelity conversion can be realized for states with small photon numbers in systems with experimentally achievable parameters. The pulsed conversion process makes it possible to maintain high conversion fidelity at elevated bath temperatures for states with small photon numbers and in systems with experimentally achievable parameters. An optomechanical interface that converts quantum states between optical fields with different wavelengths opens up a new and promising avenue for interfacing hybrid quantum systems and networks [10]. Then, Garg *et al.* presented a scheme for the adiabatic transfer of average fluctuations in the phonon number between two membranes in an optical cavity [45]. Soon after, by invariant-based inverse engineering, Chen *et al.* designed classical driving fields to transfer quantum fluctuations between two suspended membranes in an optomechanical cavity system [46]. Thus, the exchange of the energy fluctuations between two mechanical systems may pose as a possible quantum communication protocol. This clearly opens up an avenue of quantum communication between two truly mesoscopic systems.

Inspired from the previous works [10, 44–46], we propose a scheme based on Lyapunov control function V to transfer the energy fluctuations between two membranes. Different from the reported works [44–46] where a certain initial state or strict adiabatic condition is needed, Lyapunov-based control scheme could realize the energy fluctuations transfer with a random initial state. Besides, there's no requirement for the strict adiabatic condition. So the scheme is much more universal and easier to realize under the current experimental conditions.

4.1 Physical system and the derivation of effective linearized Hamiltonian

As shown in Fig. 4, the cavity optomechanical system contains a single-mode cavity of frequency ω_c and two suspended membranes. For convenience, we mark the two suspended membranes as the first and the second membrane, respectively. The decay rate and the frequency of the two membranes are $\gamma_{m,k}$ and $\omega_{m,k}$ $(k = 1, 2)$. Then, a monochromatic wave Ω is added to drive the modes a. In this case, the Hamiltonian for the system reads ($\hbar = 1$)

$$\begin{aligned} H &= H_0 + H_I + H_D, \\ H_0 &= \omega_c a^\dagger a + \sum_{k=1,2} \omega_{m,k} b_k^\dagger b_k, \\ H_I &= -g_1 a^\dagger a (b_1 + b_1^\dagger) + g_2 a^\dagger a (b_2 + b_2^\dagger), \\ H_D &= \Omega a e^{\mathrm{i}\omega_l t} + \mathrm{H.c.}. \end{aligned} \tag{10}$$

In Eq. (10), a is the annihilation operator for the cavity mode with corresponding frequency ω_c, while $b_k (k = 1, 2)$ is the annihilation operator of the mechanical mode with respective frequency $\omega_{m,k}$, and $g_1(g_2)$ determines the optomechanical coupling for the first (second) membrane with cavity mode. In the rotating frame of laser frequency

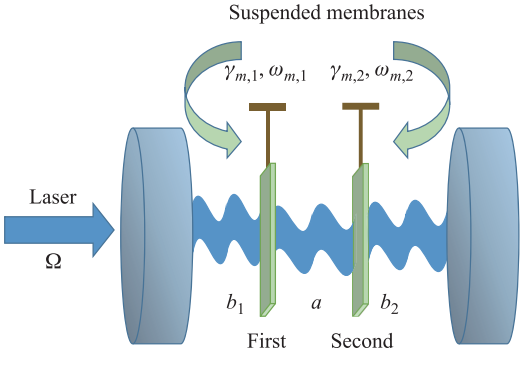

Fig. 4 Schematic diagram of two membranes inside an optical cavity. Two membrane oscillators are placed in the middle of cavity which is driven by a continuous-wave input laser, the coupling between cavity and membrane is proportional to the position of the oscillator.

($\Delta = \omega_c - \omega_l$), the Hamiltonian H takes the following form

$$\begin{aligned} H = &\Delta a^\dagger a + \Omega(a + a^\dagger) + \sum_{k=1,2} \omega_{m,k} b_k^\dagger b_k \\ &- g_1(a^\dagger a)(b_1 + b_1^\dagger) + g_2(a^\dagger a)(b_2 + b_2^\dagger). \end{aligned} \tag{11}$$

In order to study the dynamics of the cavity mode and the membranes, we use the standard linearization procedure [2], in which one expands all the bosonic operators as a sum of the average values and the zero-mean fluctuation as follows: $a \to \alpha + \delta a$ and $b_k \to \beta_k + \delta b_k$, where α and β_k are generally complex and denote the steady-state values of the annihilation operators. Then, an effective Hamiltonian for the operator fluctuations (derivation is given in Appendix C) is given as

$$H_{\text{eff}} = (-g_1\alpha^*\delta b_1^\dagger \delta a + g_2\alpha^*\delta b_2^\dagger \delta a) + \text{H.c.}, \tag{12}$$

where

$$\alpha = \frac{\Omega}{-\Delta' + \mathrm{i}\gamma/2}. \tag{13}$$

4.2 Corresponding Lyapunov control function and control fields

Based on the linearized Hamiltonian of the system in Eq. (C6) where the free (internal) Hamiltonian is $H_{0,line} = \Delta' \delta a^\dagger \delta a + \sum_{k=1,2} \omega_{m,k} \delta b_k^\dagger \delta b_k$, we utilize the Lyapunov control function $V = Tr(P\rho)$ to achieve the fluctuation transfer between membranes. The Hermitian operator P is chosen as $P = \delta b_2^\dagger \delta b_2 - \delta b_1^\dagger \delta b_1$ and the corresponding Lyapunov control function is

$$V(\rho) = Tr(\delta b_2^\dagger \delta b_2 \rho - \delta b_1^\dagger \delta b_1 \rho). \tag{14}$$

Namely, we choose the mean fluctuation excitations from mode b_2 to minus the mean fluctuation excitations from mode b_1 as the Lyapunov control function. In order to obtain the concrete expression form of effective control Hamiltonian $H_c(t)$ and design the corresponding control fields, we calculate the time derivative of V as

$$\begin{aligned} &\dot{V} = \sum_{n=1}^{k} f_n(t) T_n(t), \\ &T_n(t) = Tr\{-\mathrm{i}\rho[\delta b_2^\dagger \delta b_2 - \delta b_1^\dagger \delta b_1, H_n]\}, \\ &H_1 = -g_1\alpha^*\delta b_1^\dagger \delta a + \text{H.c.}, \\ &H_2 = g_2\alpha^*\delta b_2^\dagger \delta a + \text{H.c.}, \\ &T_1 = Tr\{-\mathrm{i}\rho(g_1\alpha^*\delta b_1 \delta a^\dagger - g_1\alpha\delta b_1^\dagger \delta a)\}, \\ &T_2 = Tr\{-\mathrm{i}\rho(-g_2\alpha^*\delta b_2 \delta a^\dagger + g_2\alpha\delta b_2^\dagger \delta a)\}. \end{aligned} \tag{15}$$

When $f_n(t)$ is chosen to keep $\dot{V} \leq 0$, the mean fluctuation excitations transfer from mode b_1 to mode b_2. After setting the time-dependent coupling strength as $f_n(t) = -KT_n(t)$ with K a positive constant, we obtain the control Hamiltonian $H_c(t)$ as

$$\begin{aligned} H_c(t) &= \sum_{n=1}^{k} f_n(t) H_n \\ &= -KT_1H_1 - KT_2H_2. \end{aligned} \tag{16}$$

With control Hamiltonian $H_c(t)$ in Eq. (16), the mean fluctuation excitations transfer from mode b_1 to mode b_2 while V decreases to its minimum value.

4.3 Analysis and numerical simulations

In this subsection, we show in details how to transfer fluctuation excitations from mode b_1 to mode b_2 with the help of Lyapunov-based control scheme. After linearizing the Hamiltonian of the system, we only consider the average quantum fluctuation instead of the actual motion of the mechanical membranes. Assuming that the decay rates of the cavity and membranes are much smaller than their fundamental frequencies such that there is no significant decay of the photons during the transfer process. (We verify that the moderate values of decay rates of the subcavity modes and the membranes do not affect the transfer process much in Appendix A.)

The simulations are performed in the Fock space. For the sake of simplicity, here we also truncate the Fock space of each oscillator up to 15-Fock-states and the dissipation of each resonator is ignored. The reason is similar to that mentioned in Section 3.

Firstly, we assume the first resonator is initially in a thermal state with average phonon number $\langle n_{b_1} \rangle = 3.35$ and the auxiliary system is prepared in its ground state. For the sake of convenience, we define the final average excitation fluctuation of the second membrane $\langle \delta b_2^\dagger \delta b_2 \rangle = F$ as the fidelity of the transfer process. For each case, the control field $g(t)$ starts with a nonzero small number to avoid $f_n(t)$ at the initial time.

With suitable parameters, the Lyapunov-based control fields versus time are shown in Fig. 5. From Fig. 5 we can see that with the evolution going on, the control function $f_1(t)(f_2(t))$ gradually decreases and finally disappears at the end of the evolution. This condition guarantees the stability of the system because the control fields will vanish after a spell of time. Finally, the system is only affected by the original Hamiltonian H_{eff}.

As shown in Fig. 6, we display the evolution of the average excitation fluctuations of the two membranes by solving numerically the Langevin equations. The fluctuation in the first membrane is gradually transferred to the second one after we apply the Lyapunov-based control fields in Eq. (16) to the system. Such a transfer of fluctuations between two membranes is not perfect because we should take the effect caused by time delay into consideration.

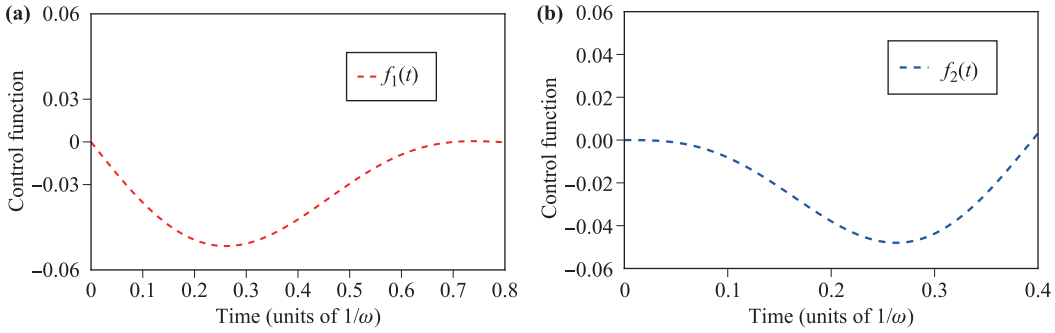

Fig. 5 The Lyapunov-based control functions versus time. **(a)** The control function $f_1(t)$ versus time. **(b)** The control function $f_2(t)$ versus time. The control fields are switched off when b_2 mode is equal to 0.99. The corresponding parameters are $\omega = 50\,\mathrm{MHz}$, $\omega_{m,1} = \omega_{m,2} = \omega$, $\Delta^{'} = 2\omega$, $g_1 = g_2 = 0.05\omega$, $K = 0.01$, and $\Omega = 50\omega$.

4.4 Time delay effect

In this subsection, we should take the non-negligible (positive or negative) time delay into consideration for better practical implementation of the scheme. Here we set these time delays may stem from actuators and electronic devices in the control loop [68].

Consider a cavity optomechanics system with a free evolution Hamiltonian $H_{0,delay}$ and a control Hamiltonian $H_{c,delay}$. For the sake of generality, the free Hamiltonian $H_{0,delay}$ can be written as

$$H_{0,delay} = \sum_{j}^{\infty} \delta a^{\dagger} \delta a + \sum_{j}^{\infty} \omega_{m,j} \delta b_j^{\dagger} \delta b_j. \tag{17}$$

Then we choose the target state as the ground state $|\phi\rangle$ of $H_{0,delay}$. The control Hamiltonian $H_{c,delay}$ is fully connected, which means for any m and n, we have $\langle\phi_n|H_{c,delay}|\phi_m\rangle \neq 0$.

It is obvious that the controlled dynamic is affected by the delay through the control field $f(t-\tau)$ significantly. In this case, the control problem would be much more complex and difficult to solve than that without time delay. Thus, we shall use the control fidelity defined by $F = \langle \delta b_2^{\dagger} b_2 \rangle$ to quantify the effect caused by time delay. After taking the time delay into consideration, the control fidelity F becomes a function of the delay time τ. When the delay time τ is small enough to be viewed as perturbation, the fidelity can be expanded up to the second order in τ as $F(t,\tau) = F(t,\tau=0) + \frac{\partial F(t,\tau)}{\partial \tau}|_{\tau=0} \cdot \tau + \frac{1}{2}\frac{\partial^2 F(t,\tau)}{\partial \tau^2}|_{\tau=0} \cdot \tau^2 + \cdots$ [69]. Here we should notice that the delay time τ only connects with the control field $f_n(t)$, so we further simplify the function of the control fidelity F and have $\frac{\partial F}{\partial \tau} = \frac{\partial F}{\partial f}\frac{\partial f}{\partial \tau}$ and $\frac{\partial^2 F}{\partial \tau^2} = \frac{\partial^2 F}{\partial f^2}\frac{\partial f^2}{\partial \tau^2}$. Considering that $\frac{\partial F}{\partial f}$ remains unchanged for the control system regardless of the time delay, so we find $\frac{\partial f}{\partial \tau}$ plays a crucial role in the time delay effects. With a small time delay τ, the control field $f(t-\tau)$ can be expanded up to second order in τ^2 as $f(t-\tau) \approx f(t) - \frac{\partial f(t)}{\partial t}\tau + \frac{1}{2}\frac{\partial^2 f(t)}{\partial t^2}\tau^2$. It is obvious that in the presence of time delay, the final control fidelity depends not only on the delay time, but also on the initial states. The control fidelity is sensitive to the time delays so it is quite a challenge to realize the perfect fluctuation transfer between membranes with Lyapunov-based control scheme when we take the time delay into consideration [69].

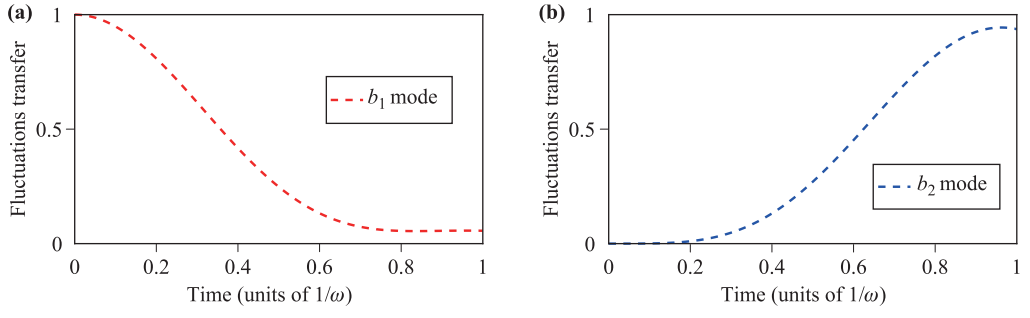

Fig. 6 **(a)** The average excitation fluctuations of the first membrane b_1 versus time when we use the Lyapunov-based control scheme. **(b)** The average excitation fluctuations of the second membrane b_2 versus time when we use the Lyapunov-based control scheme. The corresponding parameters are $\omega = 50\,\mathrm{MHz}$, $\omega_{m,1} = \omega_{m,2} = \omega$, $\Delta^{'} = 2\omega$, $g_1 = g_2 = 0.05\omega$, $K = 0.01$, and $\Omega = 50\omega$.

5 Bang–bang solutions of control fields' waveform

5.1 The bang–bang design of waveform

In the Lyapunov-based control scheme, the amplitude of the control fields $f_n(t)$ is proportional to $T_n(t)$ and will still change during the whole evolution process. For better practical implementation of the scheme, we need to manipulate the control fields at each instance of time and compensate the positive or negative effect caused by time delay in experiments. Therefore, this kind of amplitude may be difficult to control in realistic situations and errors would be introduced in the complexity regulation because the control fields are a continuous function of time. Thus, this is a challenging task for practical applications. One solution to this problem is to replace the control field by a square pulse train called bang–bang control fields.

Bang–bang control is a kind of feedback control method that switches suddenly between two states. Because of simplicity or convenience, bang–bang solutions are ubiquitous with applications including atom cooling [70, 71], transport of trapped-ion qubits [72–74], ground-state preparation [75], and so on. Besides, this method can be further extended to solve other problems such as the simplification of control fields' waveform. In this case, the bang–bang control is restricted to switch suddenly between a lower bound and an upper bound. Therefore, we try to use the bang–bang solutions to simplify the Lyapunov control fields and call the optimized fields as optimized bang–bang control fields. Similar to Ref. [63], we consider the following factors about the amplitude of the control fields$f_n(t)$: (i) Weak amplitude would lead to long evolution time. (ii) Strong external control fields may destroy the approximate condition. (iii) Strong fields may disturb neighboring quantum systems that we do not want to be involved in. Based on these factors, we set a constraint on the strength of each field as Q, and the simplified control fields become [63]

$$f_n(t) = \begin{cases} -Q & (T_n(t) > 0), \\ Q & (T_n(t) < 0), \\ 0 & (T_n(t) = 0). \end{cases} \tag{18}$$

After using the corresponding bang–bang optimization process in Eq. (18) to modify the Lyapunov control field's waveform, the simplified control Hamiltonian $H_c(t)$ becomes

$$H_c(t) = \begin{cases} -QH_1 - QH_2 & (T_n(t) > 0), \\ QH_1 + QH_2 & (T_n(t) < 0), \\ 0 & (T_n(t) = 0). \end{cases} \tag{19}$$

This design has the bang–bang type waveform and may be easy to realize experimentally [69]. The unwilling effect caused by time delay is successfully eliminated because there is no need to change the amplitude of the control fields at each instance of time. Besides, the bang–bang-based control scheme could maximize the use of energy because the strength of each field is always at the max constraint value $|Q|$ during the whole evolution. Therefore, we cannot help but wonder if the optimized bang–bang control fields could effectively shorten the time of evolution. In order to find the answer, we use bang–bang-based control scheme to realize the fluctuation transfer between membranes and make a comparison between the optimized bang–bang control fields and the Lyapunov control fields in the following numerical simulation.

5.2 Analysis and numerical simulations

In this subsection, we first show in details how to transfer fluctuation excitations from mode b_1 to mode b_2 with the help of bang–bang-based control scheme. Then, in order to find out whether the bang–bang-based control scheme has an advantage in terms of evolution rate, we make a comparison between the transfer effects caused by the bang–bang-based control scheme and by the Lyapunov-based control scheme.

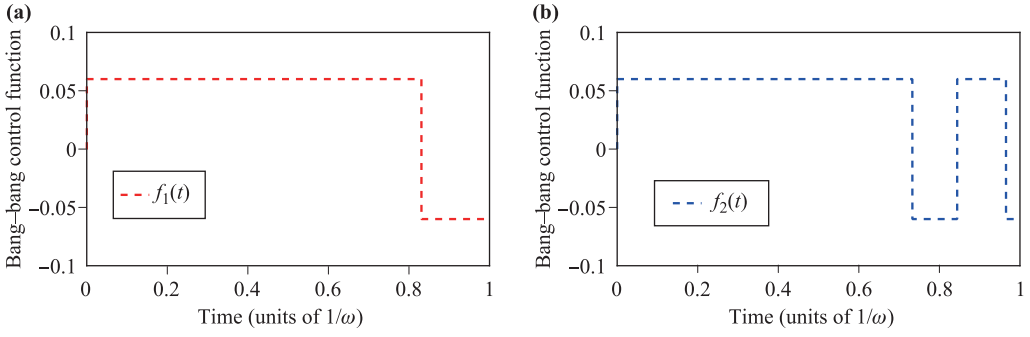

Fig. 7 The optimized bang–bang control functions versus time. **(a)** The control function $f_1(t)$ versus time. **(b)** The control function $f_2(t)$ versus time. The control fields are switched off when b_2 mode is equal to 0.99. The corresponding parameters are $\omega = 50\,\mathrm{MHz}$, $\omega_{m,1} = \omega_{m,2} = \omega$, $\Delta' = 2\omega$, $g_1 = g_2 = 0.05\omega$, $K = 0.01$, and $\Omega = 50\omega$.

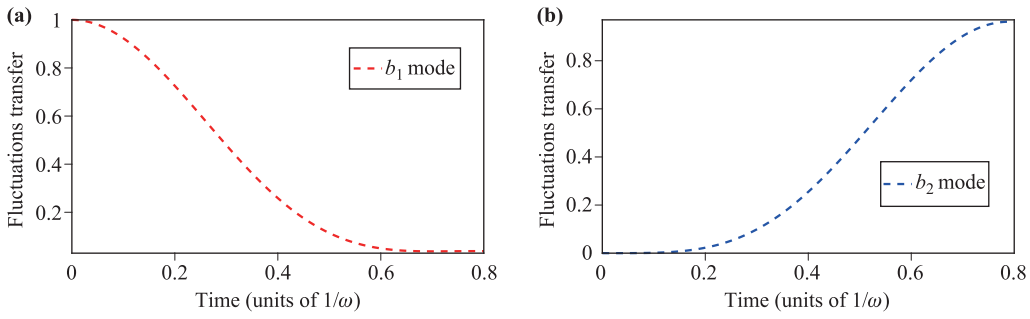

Fig. 8 **(a)** The average excitation fluctuations of the first membrane b_1 versus time when we use the bang–bang-based control scheme. **(b)** The average excitation fluctuations of the second membrane b_2 versus time when we use the bang–bang-based control scheme. The corresponding parameters are $\omega = 50\,\mathrm{MHz}$, $\omega_{m,1} = \omega_{m,2} = \omega$, $\Delta^{'} = 2\omega$, $g_1 = g_2 = 0.05\omega$, $K = 0.01$, and $\Omega = 50\omega$.

Similar to that in Section 4, the simulations are performed in the Fock space. Firstly, we assume the first resonator b_1 is initially in a thermal state with average phonon number $\langle n_{b_1} \rangle = 3.35$ and the auxiliary system is prepared in its ground state. For the sake of convenience, we define the final average excitation fluctuation of the second membrane $F = \langle \delta b_2^{\dagger} b_2 \rangle$ as the fidelity of the transfer process. For each case, the control field $g(t)$ starts with a nonzero small number to avoid $f_n(t)$ at the initial time.

As shown in Fig. 7, the optimized bang–bang control fields have the bang–bang waveform with maximum strength $Q = 0.06$. (According to Fig. 5, the strength of each control field is no more than 0.06 so we set the maximum strength of each field as $|Q| = 0.06$.) The strength of each field is always at the max constraint value $|Q| = 0.06$ during the whole evolution, so the optimized bang–bang control fields make full use of control fields' energy and are easy to realize experimentally. When the final average excitation fluctuation of the second membrane $F = \langle \delta b_2^{\dagger} b_2 \rangle$ is larger than 0.99, we turn off the control fields and the system becomes stable.

After optimizing the control fields, in order to learn about the fluctuation transfer effect of the bang–bang-based control scheme, we simulate the evolution of the average excitation fluctuations of the two membranes by solving numerically the Langevin equations. As shown in Fig. 8, complete fluctuation transfer between membranes can be achieved. The fluctuation in the first membrane is gradually transferred to the other one after we apply the bang–bang-based control fields in Eq. (19) to the system.

Noted that when the evolution arrives $t = 0.8$, the modes b_1 and b_2 almost reach 0 and 1, respectively, which means the process of transfer has basically completed. There is no need of the further change of $f_2(t)$. Meanwhile, when the system is near the target state, the control fields almost makes no sense to the evolution. So we can add a judgment statement when we write the code, if the the mode $b_2 > 0.99$, we turn off the control fields $f_1(t)$ and $f_2(t)$ and the fluctuation transfer is obtained.

In the following, in order to demonstrate the advantages of the bang–bang-based control scheme over the traditional one, we display the average excitation fluctuations of the second membrane for these two kinds of control scheme in Fig. 9.

Figure 9 shows that while the blue dotted line reaches 1, the red solid line only reaches 0.7. It is obvious that once we use the bang–bang-based control scheme, the efficiency of fluctuation transfer has been significantly improved, compared with the Lyapunov-based control scheme. Because the bang–bang-based control scheme leads to a faster decrease of Lyapunov control function V and the system will evolve to the target state with a faster evolution speed. Besides, the optimized bang–bang control fields are easy to realize in current experiments without causing operational errors. So it is seen that the simplified control fields can be a good candidate for realistic experimental environment.

Interestingly, when we use the optimized bang–bang control fields to drive the system, these control fields may oscillate with very high frequency at the end of evolution. These oscillations are closely associated with the initial state, the strength of control fields, and the distance be-

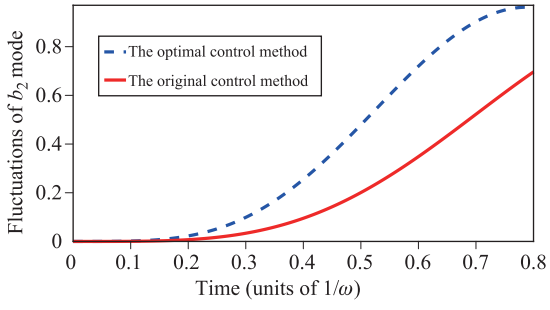

Fig. 9 The evolutions of bang–bang-based control scheme and Lyapunov-based control scheme. The corresponding parameters are $\omega = 50\,\mathrm{MHz}$, $\omega_{m,1} = \omega_{m,2} = \omega$, $\Delta^{'} = 2\omega$, $g_1 = g_2 = 0.05\omega$, $K = 0.01$, and $\Omega = 50\omega$.

tween the actual and target states. In bang–bang-based control scheme, $f_n(t)$ is designed to take the value Q or $-Q$, which makes the state oscillate at almost every step of simulation. While in Lyapunov-based control scheme, the control field $f_n(t)$ decreases to zero with $T_n(t) \to 0$. Nevertheless, this problem can be solved by averaging the control fields over a proper time period and using the reshaped fields instead of the oscillating one [63]. By doing so, the same control fields and results would be obtained.

6 Conclusion

In this paper, we have proposed a quantum control scheme based on Lyapunov control function V. To demonstrate the effectiveness of Lyapunov-based control scheme, we realize the cooling of mechanical oscillator in LC circuit and successfully transfer the fluctuation between membranes without meeting strict adiabatic conditions or specific initial state in cavity optomechanics system. The simulations show that the implementation of Lyapunov-based control scheme will drive the system gradually to evolve to the target state with the decrease of Lyapunov control function V. However, in the Lyapunov-based control scheme, the amplitude of the control fields $f_n(t)$ is proportional to $T_n(t)$ and will change during the evolution. To realize such fields in experiments, we need to manipulate the control fields at each instance of time and compensate the positive or negative effects caused by time delay. Therefore, we try to use the bang–bang solutions to simplify the control fields. Some optimizations are made on the Lyapunov-based control waveform and the bang–bang-based control scheme makes Lyapunov control function V decrease faster. So the evolution time is effectively reduced. In addition to this, the optimized design of control fields makes this scheme easier to implement under current experimental conditions because the unwilling effect caused by time delay is successfully eliminated. There is no need to change the amplitude of the control fields at each instance of time so the errors introduced in the complexity regulation could be reduced.

It is worth emphasizing that the control theory is not limited to cooling of the resonators and the fluctuation transfer between membranes, and can also be utilized to study the actual motion of the mechanical membranes and other quantum information tasks. Hence, we hope that the work may open a new avenue of the experimental realization of cooling mechanical oscillator, quantum fluctuations transfer between membranes and other quantum information tasks in the near future.

Acknowledgements This work was supported by the National Natural Science Foundation of China under Grant Nos. 11575045, 11874114, and 11674060, the Natural Science Funds for Distinguished Young Scholar of Fujian Province under Grant No. 2020J06011, Project from Fuzhou University under Grant JG202001-2, the Natural Science Foundation of Fujian Province under Grant No. 2018J01414, and the China Postdoctoral Science Foundation under Grant No. 2021M691150.

Appendices

A The derivation about the effect of decay rates of the cavity modes and the membranes

The Langevin equations for the operator fluctuations can be obtained as

$$\begin{aligned}
\delta\dot{a} &= \mathrm{i}g_1\alpha\delta b_1 - \mathrm{i}g_2\alpha\delta b_2 - \gamma/(2\delta a) + \sqrt{\gamma}\delta a^{in},\\
\delta\dot{b_1} &= \mathrm{i}g_1\alpha\delta a - \gamma_{m,1}/(2\delta b_1) + \sqrt{\gamma_{m,1}}\delta b_1^{in},\\
\delta\dot{b_2} &= -\mathrm{i}g_2\alpha\delta a - \gamma_{m,2}/(2\delta b_2) + \sqrt{\gamma_{m,2}}\delta b_2^{in}.
\end{aligned} \tag{A1}$$

The above equation can be written in a matrix form as $\mathrm{i}\dot{F} = MF$, where $F = \left(\delta a \;\; \delta b_1 \;\; \delta b_2\right)^{\mathrm{T}}$ and $M = \begin{pmatrix} -\mathrm{i}\frac{\gamma}{2} & g_1\alpha & -g_2\alpha \\ g_1\alpha & -\mathrm{i}\frac{\gamma_{m,1}}{2} & 0 \\ -g_2\alpha & 0 & -\mathrm{i}\frac{\gamma_{m,2}}{2} \end{pmatrix}$. We find that the above matrix M exhibits a zero eigenvalue, in the absence of the decay terms, with the corresponding eigenmode

$$\phi_D = (g_1\alpha)\delta b_2 - (g_2\alpha)\delta b_1. \tag{A2}$$

If we consider the damping terms of our system as a perturbation, we can obtain the deviation in the eigenvalue 1 from zero, using the first-order perturbation theory. The matrix M can be divided into two parts: one (M_{nodec}) without the decay term and the other (M_{decay}) that includes elements involving only the decay rates. In this case, $M = M_{nodec} + M_{decay}$, where $M_{decay} = -\mathrm{i}diag[\frac{\gamma}{2}\frac{\gamma_{m,1}}{2}\frac{\gamma_{m,2}}{2}]$.

So the first-order correction of the eigenvalue can be obtained as

$$\begin{aligned}
\lambda_1^{'} &= \phi_D^T M_{decay}\phi_D \\
&= -2\mathrm{i}\gamma(g_1g_2\alpha^2)^2 - \mathrm{i}\frac{\gamma_{m,1}}{2}(g_2\alpha)^2 - \mathrm{i}\frac{\gamma_{m,2}}{2}(g_1\alpha)^2,
\end{aligned} \tag{A3}$$

where the zero-eigenvalue eigenmode ϕ_D is considered in its matrix form.

Clearly this does not deviate much from the value zero. This suggests that the moderate values of decay rates of the subcavity modes and the membranes do not affect the transfer process much. The transfer is nearly complete in the presence of the decay of all the modes.

Other important works on undulation transfer also ignore the effect of dissipation because of the small effect of dissipation on the fluctuation transfer [45, 46].

B Detecting the fluctuations of the mechanical membrane

The fluctuation of the mechanical membrane is not easy to detect because it is quite tiny. However, detecting the fluctuations of the mechanical membrane is achievable. Some important work has been proposed or discussed on how to detect the fluctuations of the mechanical membrane and resonators [76–78].

Vitali *et al.* showed how stationary entanglement between an optical cavity field mode and a macroscopic vibrating mirror can be generated by means of radiation pressure [76]. They also showed how the generated optomechanical entanglement can be quantified, and suggested an experimental readout scheme to fully characterize the entangled state. They discussed the experimental detection of the generated optomechanical entanglement. In order to measure E_N at the steady state, one has to measure all ten independent entries of the correlation matrix V. This has been recently experimentally realized for the case of two entangled optical modes at the output of a parametric oscillator. In this case, the measurement of the field quadratures of the cavity mode can be straightforwardly performed by homodyning the cavity output using a local oscillator with an appropriate phase. Measuring the mechanical mode is less straightforward. However, they considered a second Fabry–Perot cavity C2, adjacent to the first one and formed by the movable mirror and a third fixed mirror (see Fig. S1), it is possible to adjust the parameters of C2 so that both the position and the momentum of the mirror can be measured by homodyning the C2 output. By changing the phases of the two local oscillators and by measuring the correlations between the two cavity outputs, one can determine all of the entries of the CM V and from them numerically extract the logarithmic negativity E_N. Chiara *et al.* studied a device formed by a Bose–Einstein condensate (BEC) coupled to the field of a cavity with a moving end mirror and found a working point such that the mirror-light entanglement is reproduced by the BEC-light quantum correlations [78]. This provided an experimentally viable tool for inferring mirror-light entanglement with only a limited set of assumptions. They proved the existence of tripartite entanglement in the hybrid device, persisting up to temperatures of a few milli-Kelvin, and discussed a scheme to detect it.

From the above works we can see that detecting the fluctuations of the mechanical membrane is not easy but achievable.

C Derivation of effective Hamilton in Eq. (14)

Using the above Hamiltonian in Eq. (11) and the input-output formalism [45, 46], we obtain the following set of Langevin equations for the relevant operators

$$\begin{aligned}\dot{a} &= -(\gamma/2+\mathrm{i}\Delta)a+\mathrm{i}g_1a(b_1+b_1^\dagger)-\mathrm{i}g_2a(b_2+b_2^\dagger)\\ &\quad-\sqrt{\gamma}a^{in},\\ \dot{b}_1 &= -(\gamma_{m,1}/2+\mathrm{i}\omega_{m,1})b_1+\mathrm{i}g_1(a^\dagger a)+\sqrt{\gamma_m}b_1^{in},\\ \dot{b}_2 &= -(\gamma_{m,2}/2+\mathrm{i}\omega_{m,2})b_2-\mathrm{i}g_2(a^\dagger a)+\sqrt{\gamma_m}b_2^{in},\end{aligned} \tag{C1}$$

where γ is the decay rate of the cavity and $\gamma_{m,k}$ $(k=1,2)$ is the dissipation rate of the kth membrane. The noise operators a^{in} and b_k^{in} satisfy

$$\begin{aligned}&\langle a^{in}(t)a^{\dagger in}(t')\rangle=\delta(t-t'),\\ &\langle a^{\dagger in}(t)a^{in}(t')\rangle=0,\\ &\langle b_k^{in}(t)b_k^{\dagger in}(t')\rangle=(\bar{n}_{th}+1)\delta(t-t'),\\ &\langle b_k^{\dagger in}(t)b_k^{in}(t')\rangle=(\bar{n}_{th})\delta(t-t'),\end{aligned} \tag{C2}$$

where $\bar{n}_{th}=\exp[\hbar\omega_{m,k}/(k_BT)]^{-1}$ is the mean thermal excitation number in the bath, interacting with the mechanical oscillator with frequency $\omega_{m,k}$ at an equilibrium temperature T and k_B is the Boltzmann constant.

In order to study the dynamics of the cavity mode and the membranes, we use the standard linearization procedure [2], in which one expands all the bosonic operators as a sum of the average values and the zero-mean fluctuation as follows: $a\to\alpha+\delta a$ and $b_k\to\beta_k+\delta b_k$, where α and β_k are generally complex and denote the steady-state values of the annihilation operators. Applying this transformation to Eq. (C2), we obtain the following equations for the average value of the operators:

$$\begin{aligned}\dot{\alpha} &= -(\gamma/2+\mathrm{i}\Delta')\alpha-\mathrm{i}\Omega,\\ \dot{\beta}_1 &= -(\gamma_{m,1}/2+\mathrm{i}\omega_{m,1})\beta+\mathrm{i}g_1|\alpha|^2,\\ \dot{\beta}_2 &= -(\gamma_{m,2}/2+\mathrm{i}\omega_{m,2})\beta-\mathrm{i}g_2|\alpha|^2,\end{aligned} \tag{C3}$$

where $\Delta'=\Delta-g_1(\beta_1+\beta_1^*)+g_2(\beta_2+\beta_2^*)$ represents the modified detuning of the respective cavity mode. The steady-state solution for α can be found by taking the time derivatives equal to zero as follows:

$$\alpha=\frac{\Omega}{-\Delta'+\mathrm{i}\gamma/2}. \tag{C4}$$

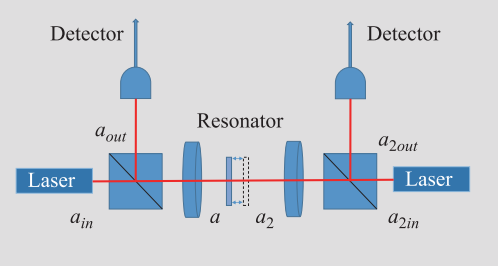

Fig. S1 Schematic description of the proposed experiment, including the second Fabry–Perot cavity on the right for the detection of the mechanical motion[76].

Similarly, the Langevin equations for the fluctuations part can be obtained using Eq. (C1) as

$$\begin{aligned}\delta\dot{a} =& -(\gamma/2+\mathrm{i}\Delta^{'})\delta a-\mathrm{i}g_1\alpha(\delta b_1+\delta b_1^{\dagger})\\ &+\mathrm{i}g_2\alpha(\delta b_2+\delta b_2^{\dagger})+\sqrt{\gamma}\delta a^{in},\\ \delta\dot{b_1} =& -(\gamma_{m,1}/2+\mathrm{i}\omega_{m,1})\delta b_1+\mathrm{i}g_1\alpha(\delta a+\delta a^{\dagger})\\ &+\sqrt{\gamma_{m,1}}\delta b_1^{in},\\ \delta\dot{b_2} =& -(\gamma_{m,2}/2+\mathrm{i}\omega_{m,2})\delta b_2-\mathrm{i}g_2\alpha(\delta a+\delta a^{\dagger})\\ &+\sqrt{\gamma_{m,2}}\delta b_2^{in}.\end{aligned} \tag{C5}$$

In order to obtain the linearized Hamiltonian of the system, we use the Eq. (C5) to retrodict the linearized Hamiltonian H_{line}

$$\begin{aligned}H_{line} =& \Delta^{'}\delta a^{\dagger}\delta a+\sum_{k=1,2}\omega_{m,k}\delta b_k^{\dagger}\delta b_k\\ &-g_1(\alpha^{*}\delta a+\alpha\delta a^{\dagger})(\delta b_1+\delta b_1^{\dagger})\\ &+g_2(\alpha^{*}\delta a+\alpha\delta a^{\dagger})(\delta b_2+\delta b_2^{\dagger}).\end{aligned} \tag{C6}$$

The first line of H_{line} is the unperturbed part which has no effect on the evolution, so we make a picture transform to eliminate the unperturbed part. After performing the unitary transformation $U=\exp(-\mathrm{i}H_{0,line}t)$ on Eq. (C6), where

$$H_{0,line}=\Delta^{'}\delta a^{\dagger}\delta a+\sum_{k=1,2}\omega_{m,k}\delta b_k^{\dagger}\delta b_k, \tag{C7}$$

we obtain the Hamiltonian in the interaction picture as

$$\begin{aligned}H_i =& U^{\dagger}H_{line}U\\ =& -g_1(\alpha^{*}\delta a\mathrm{e}^{-\mathrm{i}\Delta^{'}t}+\alpha\delta a^{\dagger}\mathrm{e}^{\mathrm{i}\Delta^{'}t})\\ &\cdot(\delta b_1\mathrm{e}^{-\mathrm{i}\omega_{m,1}t}+\delta b_1^{\dagger}\mathrm{e}^{\mathrm{i}\omega_{m,1}t})\\ &+g_2(\alpha^{*}\delta a\mathrm{e}^{-\mathrm{i}\Delta^{'}t}+\alpha\delta a^{\dagger}\mathrm{e}^{\mathrm{i}\Delta^{'}t})\\ &\cdot(\delta b_2\mathrm{e}^{-\mathrm{i}\omega_{m,2}t}+\delta b_2^{\dagger}\mathrm{e}^{\mathrm{i}\omega_{m,2}t}).\end{aligned} \tag{C8}$$

In order to further simplify the physical model, we choose the laser frequencies in the red sideband region $\Delta^{'}=\omega_{m,k}(k=1,2)$ and consider the weak-coupling condition [79] $\omega_{m,k}\gg|g_1\alpha|,|g_2\alpha|$. The limitations allow us to take the rotating wave approximation and obtain the final form of the effective Hamiltonian

$$H_{\mathrm{eff}}=(-g_1\alpha^{*}\delta b_1^{\dagger}\delta a+g_2\alpha^{*}\delta b_2^{\dagger}\delta a)+\mathrm{H.c.}, \tag{C9}$$

where

$$\alpha=\frac{\Omega}{-\Delta^{'}+\mathrm{i}\gamma/2}. \tag{C10}$$

References

1. T. J. Kippenberg and K. J. Vahala, Cavity optomechanics: Back-action at the mesoscale, *Science* 321(5893), 1172 (2008)
2. M. Aspelmeyer, T. J. Kippenberg, and F. Marquardt, Cavity optomechanics, *Rev. Mod. Phys.* 86(4), 1391 (2014)
3. I. Wilson-Rae, N. Nooshi, W. Zwerger, and T. J. Kippenberg, Theory of ground state cooling of a mechanical oscillator using dynamical backaction, *Phys. Rev. Lett.* 99(9), 093901 (2007)
4. Y. C. Liu, Y. F. Xiao, X. S. Luan, and C. W. Wong, Dynamic dissipative cooling of a mechanical resonator in strong coupling optomechanics, *Phys. Rev. Lett.* 110(15), 153606 (2013)
5. X. Y. Lü, Y. Wu, J. R. Johansson, H. Jing, J. Zhang, and F. Nori, Squeezed optomechanics with phase-matched amplification and dissipation, *Phys. Rev. Lett.* 114(9), 093602 (2015)
6. A. Szorkovszky, A. C. Doherty, G. I. Harris, and W. P. Bowen, Mechanical squeezing via parametric amplification and weak measurement, *Phys. Rev. Lett.* 107(21), 213603 (2011)
7. K. Jähne, C. Genes, K. Hammerer, M. Wallquist, E. S. Polzik, and P. Zoller, Cavity-assisted squeezing of a mechanical oscillator, *Phys. Rev. A* 79(6), 063819 (2009)
8. M. Asjad, G. S. Agarwal, M. S. Kim, P. Tombesi, G. D. Giuseppe, and D. Vitali, Robust stationary mechanical squeezing in a kicked quadratic optomechanical system, *Phys. Rev. A* 89(2), 023849 (2014)
9. X. L. Huang, T. Wang, and X. X. Yi, Effects of reservoir squeezing on quantum systems and work extraction, *Phys. Rev. E* 86(5), 051105 (2012)
10. L. Tian and H. L. Wang, Optical wavelength conversion of quantum states with optomechanics, *Phys. Rev. A* 82(5), 053806 (2010)
11. C. Genes, D. Vitali, P. Tombesi, S. Gigan, and M. Aspelmeyer, Ground-state cooling of a micromechanical oscillator: Comparing cold damping and cavity-assisted cooling schemes, *Phys. Rev. A* 77(3), 033804 (2008)
12. A. Nunnenkamp, K. Børkje, J. G. E. Harris, and S. M. Girvin, Cooling and squeezing via quadratic optomechanical coupling, *Phys. Rev. A* 82(2), 021806 (2010)
13. S. Mancini, D. Vitali, and P. Tombesi, Optomechanical cooling of a macroscopic oscillator by homodyne feedback, *Phys. Rev. Lett.* 80(4), 688 (1998)
14. R. W. Peterson, T. P. Purdy, N. S. Kampel, R. W. Andrews, P. L. Yu, K. W. Lehnert, and C. A. Regal, Laser cooling of a micromechanical membrane to the quantum backaction limit, *Phys. Rev. Lett.* 116(6), 063601 (2016)
15. J. Y. Yang, D. Y. Wang, C. H. Bai, S. Y. Guan, X. Y. Gao, A. D. Zhu, and H. F. Wang, Ground-state cooling of mechanical oscillator via quadratic optomechanical coupling with two coupled optical cavities, *Opt. Express* 27(16), 22855 (2019)
16. F. Marquardt, J. P. Chen, A. A. Clerk, and S. M. Girvin, Quantum theory of cavity-assisted sideband cooling of mechanical motion, *Phys. Rev. Lett.* 99(9), 093902 (2007)
17. A. H. Safavi-Naeini and O. Painter, Proposal for an optomechanical traveling wave phonon–photon translator, *New J. Phys.* 13(1), 013017 (2011)

18. K. Stannigel, P. Komar, S. J. M. Habraken, S. D. Bennett, M. D. Lukin, P. Zoller, and P. Rabl, Optomechanical quantum information processing with photons and phonons, *Phys. Rev. Lett.* 109(1), 013603 (2012)
19. M. Tsang, Cavity quantum electro-optics (II): Input-output relations between traveling optical and microwave fields, *Phys. Rev. A* 84(4), 043845 (2011)
20. X. W. Xu, Y. J. Zhao, and Y. X. Liu, Entangled-state engineering of vibrational modes in a multimembrane optomechanical system, *Phys. Rev. A* 88(2), 022325 (2013)
21. X. W. Xu, Y. X. Liu, C. P. Sun, and Y. Li, Mechanical *PT* symmetry in coupled optomechanical systems, *Phys. Rev. A* 92(1), 013852 (2015)
22. Y. D. Wang and A. A. Clerk, Reservoir-engineered entanglement in optomechanical systems, *Phys. Rev. Lett.* 110(25), 253601 (2013)
23. V. Fiore, Y. Yang, M. C. Kuzyk, R. Barbour, L. Tian, and H. Wang, Storing optical information as a mechanical excitation in a silica optomechanical resonator, *Phys. Rev. Lett.* 107(13), 133601 (2011)
24. Y. D. Wang and A. A. Clerk, Using interference for high fidelity quantum state transfer in optomechanics, *Phys. Rev. Lett.* 108(15), 153603 (2012)
25. S. S. U and A. Narayanan, Mechanical switch for state transfer in dual-cavity optomechanical systems., *Phys. Rev. A* 88(3), 033802 (2013)
26. K. C. Schwab and M. L. Roukes, Putting mechanics into quantum mechanics, *Phys. Today* 58(7), 36 (2005)
27. T. Kippenberg and K. Vahala, Cavity opto-mechanics, *Opt. Express* 15(25), 17172 (2007)
28. V. Fiore, Y. Yang, M. C. Kuzyk, R. Barbour, L. Tian, and H. L. Wang, Storing optical information as a mechanical excitation in a silica optomechanical resonator, *Phys. Rev. Lett.* 107(13), 133601 (2011)
29. Y. D. Wang and A. A. Clerk, Using interference for high fidelity quantum state transfer in optomechanics, *Phys. Rev. Lett.* 108(15), 153603 (2012)
30. S. Barzanjeh, M. Abdi, G. J. Milburn, P. Tombesi, and D. Vitali, Reversible optical-to-microwave quantum interface, *Phys. Rev. Lett.* 109(13), 130503 (2012)
31. H. K. Li, X. X. Ren, Y. C. Liu, and Y. F. Xiao, Photon-photon interactions in a largely detuned optomechanical cavity, *Phys. Rev. A* 88(5), 053850 (2013)
32. M. D. La Haye, O. Buu, B. Camarota, and K. C. Schwab, Approaching the quantum limit of a nanomechanical resonator, *Science* 304(5667), 74 (2004)
33. J. J. Li and K. D. Zhu, All-optical mass sensing with coupled mechanical resonator systems, *Phys. Rep.* 525(3), 223 (2013)
34. B. Pepper, R. Ghobadi, E. Jeffrey, C. Simon, and D. Bouwmeester, Optomechanical superpositions via nested interferometry, *Phys. Rev. Lett.* 109(2), 023601 (2012)
35. P. Sekatski, M. Aspelmeyer, and N. Sangouard, Macroscopic optomechanics from displaced single-photon entanglement, *Phys. Rev. Lett.* 112(8), 080502 (2014)
36. A. Carlini, A. Hosoya, T. Koike, and Y. Okudaira, Time-optimal quantum evolution, *Phys. Rev. Lett.* 96(6), 060503 (2006)
37. N. Khaneja, R. Brockett, and S. J. Glaser, Time optimal control in spin systems, *Phys. Rev. A* 63(3), 032308 (2001)
38. P. D' Alessandro and E. De Santis, Controlled invariance and feedback laws, *IE EE Trans. Automat. Contr.* 46(7), 1141 (2001)
39. J. P. Palao and R. Kosloff, Quantum computing by an optimal control algorithm for unitary transformations, *Phys. Rev. Lett.* 89(18), 188301 (2002)
40. M. Mirrahimi, P. Rouchon, and G. Turinici, Lyapunov control of bilinear Schrödinger equations, *Automatica* 41, 1987 (2005)
41. X. T. Wang and S. G. Schirmer, Entanglement generation between distant atoms by Lyapunov control, *Phys. Rev. A* 80(4), 042305 (2009)
42. W. Wang, L. C. Wang, and X. X. Yi, Lyapunov control on quantum open systems in decoherence-free subspaces, *Phys. Rev. A* 82(3), 034308 (2010)
43. Y. H. Chen, W. Qin, and F. Nori, Fast and high-fidelity generation of steady-state entanglement using pulse modulation and parametric amplification, *Phys. Rev. A* 100(1), 012339 (2019)
44. C. H. Dong, V. Fiore, M. C. Kuzyk, and H. Wang, Optomechanical dark mode, *Science* 338(6114), 1609 (2012)
45. D. Garg, A. K. Chauhan, and A. Biswas, Adiabatic transfer of energy fluctuations between membranes inside an optical cavity, *Phys. Rev. A* 96(2), 023837 (2017)
46. Y. H. Chen, Z. C. Shi, J. Song, and Y. Xia, Invariant-based inverse engineering for fluctuation transfer between membranes in an optomechanical cavity system, *Phys. Rev. A* 97(2), 023841 (2018)
47. Y. H. Kang, Z. C. Shi, B. H. Huang, J. Song, and Y. Xia, Deterministic conversions between Greenberger–Horne–Zeilinger states and W states of spin qubits via Lie-transform-based inverse Hamiltonian engineering, *Phys. Rev. A* 100(1), 012332 (2019)
48. Y. H. Kang and Y. Xia, Unconventional geometric phase gate of transmon qubits with inverse Hamiltonian engineering, *IE EE J. Sel. Top. Quantum Electron.* 26(3), 6700107 (2020)
49. Y. H. Kang, Z. C. Shi, B. H. Huang, J. Song, and Y. Xia, Flexible scheme for the implementation of nonadiabatic geometric quantum computation, *Phys. Rev. A* 101(3), 032322 (2020)
50. Y. H. Kang, Y. H. Chen, Z. C. Shi, B. H. Huang, J. Song, and Y. Xia, One-step implementation of *N*-qubit nonadiabatic holonomic quantum gates with superconducting qubits via inverse hamiltonian engineering, *Ann. Phys.* 531(7), 1800427 (2019)
51. Y. Wang, C. S. Hu, Z. C. Shi, B. H. Huang, J. Song, and Y. Xia, Accelerated and noise-resistant protocol of dissipation-based Knill–Laflamme–Milburn state generation with Lyapunov control, *Ann. Phys.* 531(7), 1900006 (2019)

52. Y. H. Zhou, H. Z. Shen, and X. X. Yi, Unconventional photon blockade with second-order nonlinearity, *Phys. Rev. A* 92(2), 023838 (2015)
53. Z. C. Zhang, J. C. Pei, Y. P. Wang, and X. G. Wang, Measuring orbital angular momentum of vortex beams in optomechanics, *Front. Phys.* 16(3), 32503 (2021)
54. X. B. Yan, H. L. Lu, F. Gao, F. Gao, and L. Yang, Perfect optical nonreciprocity in a double-cavity optomechanical system, *Front. Phys.* 14(5), 52601 (2019)
55. M. M. Zhao, Z. Qian, B. P. Hou, Y. Liu, and Y. H. Zhao, Optomechanical properties of a degenerate nonperiodic cavity chain, *Front. Phys.* 14(2), 22601 (2019)
56. J. H. Liu, Y. B. Zhang, Y. F. Yu, and Z. M. Zhang, Photon-phonon squeezing and entanglement in a cavity optomechanical system with a flying atom, *Front. Phys.* 14(1), 12601 (2019)
57. S. Liu, J. H. Shen, R. H. Zheng, Y. H. Kang, Z. C. Shi, J. Song, and Y. Xia, Optimized nonadiabatic holonomic quantum computation based on Förster resonance in Rydberg atoms, *Front. Phys.* 17(2), 21502 (2022)
58. Y. H. Kang, Z. C. Shi, J. Song, and Y. Xia, Heralded atomic nonadiabatic holonomic quantum computation with Rydberg blockade, *Phys. Rev. A* 102(2), 022617 (2020)
59. Y. H. Kang, Z. C. Shi, J. Song, and Y. Xia, Effective discrimination of chiral molecules in a cavity, *Opt. Lett.* 45(17), 4952 (2020)
60. D. D' Alessandro, Introduction to Quantum Control and Dynamics, Taylor and Francis Group, Boca Raton, 2007
61. Z. C. Shi, X. L. Zhao, and X. X. Yi, Robust state transfer with high fidelity in spin-1/2 chains by Lyapunov control, *Phys. Rev. A* 91(3), 032301 (2015)
62. X. X. Yi, X. L. Huang, C. F. Wu, and C. H. Oh, Driving quantum systems into decoherence-free subspaces by Lyapunov control, *Phys. Rev. A* 80(5), 052316 (2009)
63. S. C. Hou, M. A. Khan, X. X. Yi, D. Dong, and I. R. Petersen, Optimal Lyapunov-based quantum control for quantum systems, *Phys. Rev. A* 86(2), 022321 (2012)
64. J. T. Sheng, X. R. Wei, C. Yang, and H. B. Wu, Self-organized synchronization of phonon lasers, *Phys. Rev. Lett.* 124(5), 053604 (2020)
65. W. W. Zhou, S. G. Schirmer, M. Zhang, and H. Y. Dai, Bang–bang control design for quantum state transfer based on hyperspherical coordinates and optimal time – energy control, *J. Phys. A Math. Theor.* 44(10), 105303 (2011)
66. X. T. Wang, S. Vinjanampathy, F. W. Strauch, and K. Jacobs, Ultraefficient cooling of resonators: Beating sideband cooling with quantum control, *Phys. Rev. Lett.* 107(17), 177204 (2011)
67. L. Tian, Ground state cooling of a nanomechanical resonator via parametric linear coupling, *Phys. Rev. B* 79(19), 193407 (2009)
68. K. Nishio, K. Kashima, and J. Imura, Effects of time delay in feedback control of linear quantum systems, *Phys. Rev. A* 79(6), 062105 (2009)
69. X. X. Yi, S. L. Wu, C. Wu, X. L. Feng, and C. H. Oh, Time-delay effects and simplified control fields in quantum Lyapunov control, *J. Phys. At. Mol. Opt. Phys.* 44(19), 195503 (2011)
70. D. Stefanatos, J. Ruths, and J. S. Li, Frictionless atom cooling in harmonic traps: A time-optimal approach, *Phys. Rev. A* 82(6), 063422 (2010)
71. X. J. Lu, X. Chen, J. Alonso, and J. G. Muga, Fast transitionless expansions of Gaussian anharmonic traps for cold atoms: Bang–singular–bang control, *Phys. Rev. A* 89(2), 023627 (2014)
72. M. Palmero, E. Torrontegui, D. Guéry-Odelin, and J. G. Muga, Fast transport of two ions in an anharmonic trap, *Phys. Rev. A* 88(5), 053423 (2013)
73. M. Palmero, R. Bowler, J. P. Gaebler, D. Leibfried, and J. G. Muga, Fast transport of mixed-species ion chains within a Paul trap, *Phys. Rev. A* 90(5), 053408 (2014)
74. Y. C. Ding, T. Y. Huang, K. Paul, M. J. Hao, and X. Chen, Smooth bang–bang shortcuts to adiabaticity for atomic transport in a moving harmonic trap, *Phys. Rev. A* 101(6), 063410 (2020)
75. S. Balasubramanian, S. Y. Han, B. T. Yoshimura, and J. K. Freericks, Bang–bang shortcut to adiabaticity in trapped-ion quantum simulators, *Phys. Rev. A* 97(2), 022313 (2018)
76. D. Vitali, S. Gigan, A. Ferreira, H. R. Böhm, P. Tombesi, A. Guerreiro, V. Vedral, A. Zeilinger, and M. Aspelmeyer, Optomechanical entanglement between a movable mirror and a cavity field, *Phys. Rev. Lett.* 98(3), 030405 (2007)
77. C. S. Hu, Z. Q. Liu, Y. Liu, L. T. Shen, H. Z. Wu, and S. B. Zheng, Entanglement beating in a cavity optomechanical system under two-field driving, *Phys. Rev. A* 101(3), 033810 (2020)
78. G. De Chiara, M. Paternostro, and G. M. Palma, Entanglement detection in hybrid optomechanical systems, *Phys. Rev. A* 83(5), 052324 (2011)
79. L. Tian and H. L. Wang, Optical wavelength conversion of quantum states with optomechanics, *Phys. Rev. A* 82(5), 053806 (2010)